Hindawi Publishing Corporation
Journal of Applied Mathematics
Volume 2012, Article ID 246146, 19 pages
doi:10.1155/2012/246146

Research Article

Simulation of Wave Overtopping of Maritime Structures in a Numerical Wave Flume

Tiago C. A. Oliveira, Agustín Sánchez-Arcilla, and Xavier Gironella

Maritime Engineering Laboratory, Technical University of Catalonia, 08034 Barcelona, Spain

Correspondence should be addressed to Tiago C. A. Oliveira, tiago.oliveira@upc.edu

Received 19 February 2012; Revised 23 April 2012; Accepted 2 May 2012

Academic Editor: Armin Troesch

A numerical wave flume based on the particle finite element method (PFEM) is applied to simulate wave overtopping for impermeable maritime structures. An assessment of the performance and robustness of the numerical wave flume is carried out for two different cases comparing numerical results with experimental data. In the first case, a well-defined benchmark test of a simple low-crested structure overtopped by regular nonbreaking waves is presented, tested in the lab, and simulated in the numerical wave flume. In the second case, state-of-the-art physical experiments of a trapezoidal structure placed on a sloping beach overtopped by regular breaking waves are simulated in the numerical wave flume. For both cases, main overtopping events are well detected by the numerical wave flume. However, nonlinear processes controlling the tests proposed, such as nonlinear wave generation, energy losses along the wave propagation track, wave reflection, and overtopping events, are reproduced with more accuracy in the first case. Results indicate that a numerical wave flume based on the PFEM can be applied as an efficient tool to supplement physical models, semiempirical formulations, and other numerical techniques to deal with overtopping of maritime structures.

1. Introduction

Wave overtopping is one of the most important and complex physical processes in the study of wave-structure interactions. Wave overtopping of a maritime structure is a violent natural phenomenon which may affect the structural integrity of the structure and cause damage to properties and, sometimes, lives. It is a highly nonlinear problem with a free surface, and it remains a scientific and topological technical challenge because of the complex involved nonlinearities and multiplicity of scales (e.g., wave breaking, boundary induced reflection, wave transmission, wave groupiness, mean sea level variations, and so on). Such physical processes deal with large and fast-free water surface changes and sometimes with multiple water mass separation.

Nowadays, semiempirical formulations are the most employed tool by engineers and scientists to estimate overtopping rates of maritime structures. However, because of that empirical character, the application of these models is limited to a particular structural configuration and wave conditions. For example, Owen [1] developed a formulation to calculate wave overtopping on smooth or rough impermeable sloping structures with and without a berm; Franco et al. [2] presented a formulation to estimate overtopping in vertical breakwaters; Pedersen [3] described a formulation for permeable slope breakwaters with crown walls. As the majority of semiempirical formulations used in maritime engineering, the above-mentioned formulations were obtained from small-scale physical tests, therefore distorted by scale with respect to what happens in nature.

Based on these formulations, there are a range of approaches to predict overtopping that can normally be applied to particular structures represented by simplified sections. The commonly employed methods (estimating mean overtopping discharge and overtopping volume) have been derived measuring overtopping at model tests and field campaigns. These methods relate overtopping rates to the main wave and structural parameters [4], and most are based on physical model data from 2D (wave flume) and 3D (wave tank) facilities and a geometric scale in the range $1:10$ to $1:80$.

Physical tests are used not just for developing new overtopping formulations but also for assessing prototype structural problems. In physical model tests, an understanding of model and scale effects is critical for the correct representation of the phenomenon since even the correct representation in a laboratory of the desired wave conditions is a difficult task [5].

Scale effects induce errors resulting from an incorrect reproduction of viscosity forces, surface tension forces, and elasticity forces, as a consequence of the applied Froude scaling similarity. No overtopping scale effects were identified by comparing prototype and small-scale tests with vertical smooth structures [6, 7]. However, at rubble mound structures, scale effects were identified, normally measuring more overtopping in larger scales than in smaller scale models [8].

In nature, wave overtopping is an irregular process and this randomness is not always easy to simulate in the lab [9]. Waves are generated in the laboratory as random wave trains to measure many different aspects of overtopping, such as mean overtopping discharge, wave-by-wave volumes, overtopping velocities, and travel distance, as well as other interaction parameters. The detailed wave features are also important, and it is nowadays accepted that the discharge intensity of individually overtopping waves is relevant because most of the damages that have impact on persons, vehicles, and structures are caused by overtopping of large single waves [8].

In the last three decades, there have been important developments in numerical models dealing with fluid-solid interactions. This has gone in parallel with an increased study of wave-structure interaction problems in numerical flumes. A numerical wave flume intends to be an accurate representation of a physical wave flume and, thus, the corresponding physical problem. The numerical wave flumes presented in the scientific literature can be grouped based on their basic equations and numerical schemes. Examples of numerical waves flumes based on the nonlinear shallow water (NLSW) equations applied to maritime structures can be found in van Gent [10], Dodd [11], and Hu et al. [12]. Lemos [13] developed a numerical model for the study of the movement of two-dimensional waves using a volume of fluid (VOF) technique for solving Navier-Stokes equations for incompressible fluids. Van Gent et al. [14] presented a VOF model that can simulate plunging wave breaking into porous structures. Lin and Liu [15] described the development of a VOF-type model (COBRAS) based on the Reynolds-Averaged Navier-Stokes (RANS) equations to study the evolution of

wave groupiness, shoaling, and breaking in the swash zone. Lara et al. [16] have shown the ability of the COBRAS model to simulate the interaction of irregular waves with permeable slope structures. The use of the smooth particle hydrodynamics (SPH) technique in maritime engineering began at the end of the 90s [17]. Dalrymple and Rogers [18] studied the plunging wave type breaker using a model based on the SPH method. Shao et al. [19] presented an incompressible SPH model to study the interaction of waves with coastal structures. Koshizuka et al. [20] used the moving particle semi-implicit (MPS) method to study wave breaking. Oliveira et al. [21] used the particle finite element method (PFEM) as a numerical flume to study the generation of nonlinear waves by means of different paddle types.

Due to the improvements in numerical wave flumes, they have started to be considered as a possible tool to support overtopping calculations for maritime structures [22]. Numerical overtopping studies can be found in the scientific literature for numerical wave flumes based on the NLSW [12, 23], VOF [23–26], SPH [27], and MPS [28] numerical techniques.

The major objective of this work is to investigate the ability of a numerical wave flume based on the PFEM to simulate the "correct" incident wave features and the associated overtopping for maritime structures. In order to achieve this objective, numerical results for two different structures are compared to physical data. In the first case, a well-defined benchmark test of a simple low-crested structure overtopped by regular nonbreaking waves is presented, tested in the lab, and simulated in the numerical wave flume. In the second case, state-of-the-art physical experiments of a trapezoidal structure placed on a sloping beach overtopped by regular breaking waves are simulated in the numerical wave flume.

The layout of this paper is the following: Section 2 describes the numerical technique PFM. In Section 3, wave overtopping is studied for a low-crested structure and a well-defined benchmark test case is presented. In Section 4 wave overtopping is studied for a breaking wave case. The paper ends with some conclusions and recommendations for further research.

2. The Particle Finite Element Method

The PFEM is now a well-known method in the scientific literature [29–31]. However, some specific key features of the PFEM are also included in this paper for completeness. The PFEM solves the fluid mechanics equations by a Lagrangian approach. It is a particular class of Lagrangian flow formulations, developed to solve free surface flow problems involving large deformations of the free surface, as well as the interaction with rigid bodies. The finite element method (FEM) is used to solve the continuum equations in the fluid and solid domains. The PFEM treats the mesh nodes in the fluid and solid domains as particles, which can freely move and even separate from the main fluid domain representing, for instance, the effect of water drops or melted zones. The data between two consecutive time steps is only transferred through nodes, because elements are created again at every time step by a remeshing process with new connectivities.

In the PFEM, the mass conservation and momentum conservation equations (Navier-Stokes) in the final x_i position are written as follows:

$$\frac{D\rho}{Dt} + \rho \frac{\partial u_i}{\partial x_i} = 0, \tag{2.1}$$

$$\rho \frac{Du_i}{Dt} = -\frac{\partial}{\partial_{x_i}} p + \frac{\partial}{\partial_{x_j}} \tau_{ij} + \rho f_i, \tag{2.2}$$

where ρ is the density, u_i are the Cartesian components of the velocity field, p the pressure, τ_{ij} the deviatoric stress tensor, f_i the source tensor (usually the gravity), D/Dt represents the total or material time derivate.

For Newtonian fluids, the stress tensor τ_{ij} may be expressed as a function of the velocity field through the viscosity μ by:

$$\tau_{ij} = \mu\left(\frac{\partial u_i}{\partial_{x_j}} + \frac{\partial u_j}{\partial_{x_i}} - \frac{2}{3}\frac{\partial u_l}{\partial_{x_l}}\delta_{ij}\right). \tag{2.3}$$

For near incompressible flows, $\partial u_i/\partial x_i \ll \partial u_k/\partial x_l$, and thus

$$\frac{2\mu}{3}\frac{\partial u_l}{\partial_{x_l}} \approx 0. \tag{2.4}$$

Then, the stress tensor τ_{ij} can be written as

$$\tau_{ij} \approx \mu\left(\frac{\partial u_i}{\partial_{x_j}} + \frac{\partial u_j}{\partial_{x_i}}\right). \tag{2.5}$$

Using (2.5) and after some manipulations [29], the momentum conservation equation can be finally written as

$$\rho\frac{Du_i}{Dt} \approx -\frac{\partial}{\partial_{x_i}}p + \mu\frac{\partial}{\partial_{x_j}}\left(\frac{\partial u_i}{\partial_{x_j}}\right) + \rho f_i. \tag{2.6}$$

Traditionally, computational fluids dynamics problems have been solved by models based on Eularian or ALE formulations. In Eulerian formulations, the nonlinearity is explicitly presented in the convective terms. In the PFEM Lagrangian formulation, the nonlinearity is due to the fact the momentum equation is written in the final positions of the particles.

The Navier-Stokes equations are time dependent, and thus a temporal integration needs to be carried out. The fractional-step method proposed in Codina [32] is used in PFEM for the time solution. Even when using an implicit time integration scheme, incompressibility introduces some wiggles in the pressure solution which must be stabilized to avoid pressure oscillations in some particular cases. In the PFEM, a simple and effective procedure to derive a stabilized formulation for incompressible flows based on the so-called finite calculus (FIC) formulations [33] is used.

In order to solve the governing equations that represent the continuum, particles must be connected. A mesh discretizing the fluid and solid domains must be generated in order to solve the governing equations for both the fluid and solid problems in the standard FEM fashion. A fast regeneration of the mesh at every time step on the basis of the position of the nodes in the space domain is used. A mesh is generated at each time step using the so-called extended Delaunay tessellation (EDT) [34]. The EDT allows the generation of nonstandard meshes combining elements of arbitrary polyhedrical shapes (triangles, quadrilaterals, and other polygons in the 2D case) in a computing time of order n, where n is the total number of nodes in the mesh. One of the keys to solve a fluid mechanics problem using a Lagrangian

formulation is to generate efficiently the shape functions to approximate the spatial unknown. In the PFEM, the interpolation function used by the meshless finite element method (MFEM) [35] is applied. EDT together with the MFEM is the main key to make the PFEM a useful tool.

The CPU required for meshing grows linearly with the number of nodes. However, Oñate et al [31] found that the CPU time for solving the equations exceeds that required for meshing as the number of nodes increases. As in the standard FEM, the quality of the numerical solution depends on the discretization chosen. Adaptive mesh refinements techniques can be used to improve the solution in zones of special interest.

It must be noted that the information in the PFEM is typically nodalbased, that is, the element mesh is mainly used to obtain the values of the state variables (i.e., velocities, pressure, viscosity, etc.) at the nodes. A difficulty arises in the identification of the boundary of the domain from a given collection of nodes. Indeed, the boundary can include the free surface in the fluid and the individual particles moving outside the fluid domain. For this purpose the Alpha Shape technique [36] has been used to identify the boundary nodes.

In summary, the main difference between the PFEM and the classical FEM is the remeshing technique and the evaluation of the boundary position at each time step. The rest of steps in the computation are equivalent to those of the classical FEM.

3. Overtopping of Nonbreaking Waves at a Low Crested Structure

To evaluate the performance and robustness of a numerical flume to simulate a specific physical process, it is necessary to have a theoretical model or experimental data set that can represent it. Without this information, we have no way of comparison and no way to make sure the numerical flume is really representing the true behavior. Moreover, this information is important for a previous understanding of the physical processes involved in the numerical simulation and for the preparation of the numerical model setup. Due to the complexity of the physical processes involved in wave-structure interaction, there is nowadays no theoretical model available to represent all of these problems and associated scales. Thus, if an accurate evaluation of a numerical flume is desired, high-quality physical data is necessary. However, the more complex physical tests do not always provide the best data to calibrate and improve numerical flumes. The main reason for this fact is that, when the physical tests complexity increases, the understanding of the physical processes diminishes and the control of boundary conditions also increases.

In this work, a well-defined benchmark test case was created to be tested in a physical and easily be subsequently reproduced in a numerical wave. The goal of this benchmark test is to study wave overtopping for regular nonbreaking waves at a simple, low-crested, maritime structure. Figure 1 shows the low-crested structure as well the flume configuration for which it will be tested. In this case, the model can be considered impermeable, and its layout can be defined by just five points (P1–P5 in Figure 1). The position, relative to the wave paddle, of the five layout representative points can be found in Table 1.

The low-crested structure benchmark test was reproduced in a small-scale physical wave flume. The experiments were carried out at the Maritime Engineering Laboratory (LIM) of the Technical University of Catalonia BarcelonaTech (UPC-BarcelonaTech). The flume is 18 m long, 0.4 m wide, and 0.6 m deep and is provided with a piston-type wave paddle capable of generating both regular and irregular waves. At the experiments, the water depth was kept constant ($h = 0.19$ m) from the wavemaker until the structure. Six resistance wave gauges were used to measure free surface evolution at six different points along the flume. A sampling rate of 100 Hz was used. The level of accuracy of these sensors is about 0.001 m.

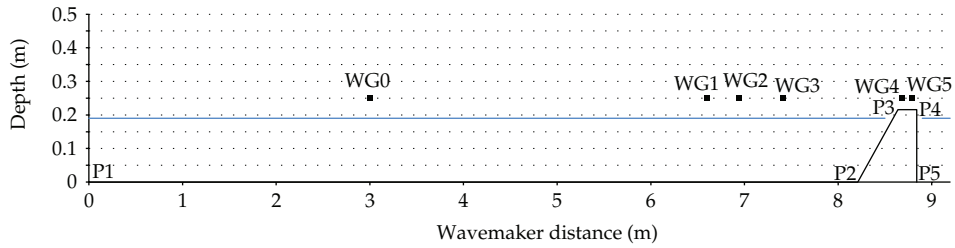

Figure 1: Sketch of CIEMito wave flume used to reproduce and understand overtopping at a low-crested maritime structure.

Table 1: Model coordinates (see Figure 1).

Point	x (m)	y (m)
P1	0.00	0.000
P2	8.21	0.000
P3	8.64	0.216
P4	8.84	0.216
P5	8.84	0.000

The free surface sensors are represented in Figure 1, and their positions can be obtained from Table 2.

This simple low-crested structure was tested for two regular wave conditions. Wave case number 1 corresponds to a wave height of $H = 0.06$ m and a wave period of $T = 1.55$ s. Wave case number 2 corresponds to a wave height of $H = 0.07$ m and a wave period of $T = 1.8$ s. Relatively mild energetic wave conditions were chosen to induce less violent and easier to understand overtopping, from which the different process and scales over the structure could be assessed.

For each wave case, two wave trains were generated. One wave ramp before and other after were added to the two desired waves trains time series. The first wave ramp objective is to slowly increase the wavemaker stroke at startup until it reaches its desired value. Wave ramps avoid unwanted large waves considered as a transient response associated with the starting and stopping of the wavemaker [5]. Paddle displacement was calculated by first order wavemaker theory as proposed by Biésel and Suquet [37]. Taking into account wave ramps, the paddle displacement can be written as

$$X_0(t) = \left(H \left(\frac{\sinh 2k_0h + 2k_0h}{8\sinh^2 k_0h} \right) \sin wt \right) \frac{t}{T} \quad \text{for } 0 < t \le T$$

$$X_0(t) = H \left(\frac{\sinh 2k_0h + 2k_0h}{8\sinh^2 k_0h} \right) \sin wt \quad \text{for } T < t \le 3T \tag{3.1}$$

$$X_0(t) = \left(H \left(\frac{\sinh 2k_0h + 2k_0h}{8\sinh^2 k_0h} \right) \sin wt \right) \left(1 - \frac{t - 3T}{T} \right) \quad \text{for } 3T < t \le 4T,$$

where H is the wave height, T is the wave period, h is the water depth in front of the paddle, k_0 is the wave number ($k_0 = 2\pi/L$), w is the angular frequency ($w = 2\pi/T$), t is the time, and L is the wavelength ($L = \tanh(2\pi h/L)gT^2/2\pi$).

Table 2: Free-surface sensor positions (see Figure 1).

Free surface sensor	Wave maker distance (m)
WG0	3.00
WG1	6.60
WG2	6.95
WG3	7.42
WG4	8.69
WG5	8.79

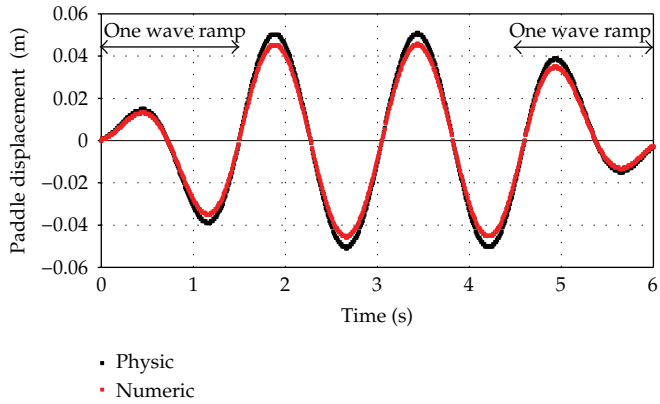

Figure 2: Physical and numerical paddle displacements for wave case 1 defined by $H = 0.06$ m and $T = 1.55$ s.

The benchmark test was simulated in a numerical wave flume based on the 2DV Navier-Stokes equations solved by the particle finite element method. To discretize the flume domain, two different nodal distances were considered. In the constant water depth zone, a 0.01 m nodal distance was selected. Around the structure, 0.005 m distance between nodes was considered. This domain discretization leads to an initial finite elements mesh of 20675 nodes. The maximum time step used in the simulations was 0.001 s. The numerical tests were run on a 2.67 GHz Intel Core i7 CPU920. For these conditions, the numerical wave flume took about 50 hours to simulate 20 s of physical model test.

Other time and mesh resolutions were tested in order to evaluate the computational time and the accuracy of the results along the flume. It was found that the accuracy of the overtopping results decreases substantially for nodal distances around the structure greater than 0.005 m.

In the numerical wave flume, waves were generated as similar as possible to those generated in the physical flume. A numerical piston paddle moving according the physical piston paddle was simulated. This boundary condition is solved by PFEM as a solid-liquid interaction problem. Although the physical flume can be considered as a 2DV problem, there are some 3D effects close to wavemaker (recirculation, water losses, etc.) that a 2DV numerical flume does not take into account. The main difference is that, in the physical flume, there is a water flux between the back and front sides of the paddle due to the leakage between the paddle and the walls of the flume; this cannot be easily simulated in a 2D numerical flume.

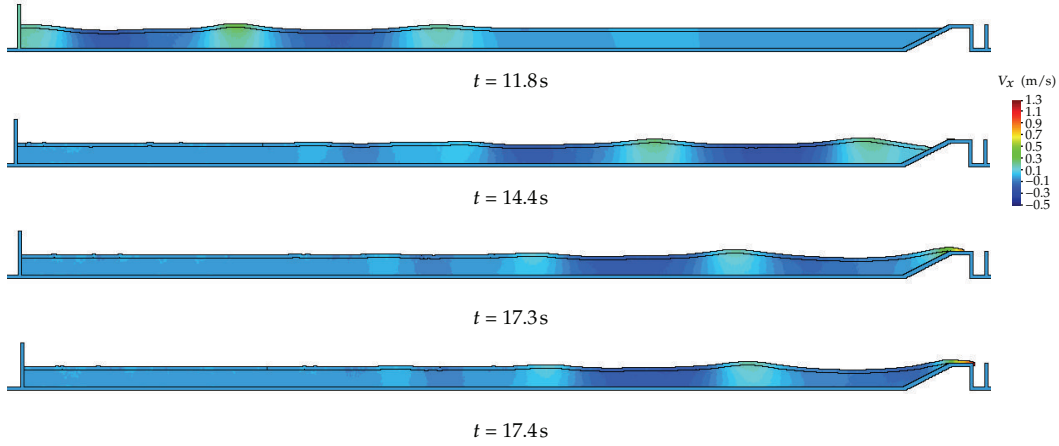

Figure 3: Horizontal velocities (m/s) along the flume for four different time steps and for wave case 1, $H = 0.06$ m and $T = 1.55$ s.

Madsen [38] proposed that the leakage around the piston will decrease the amplitude of the generated waves by an amount Δa which may be found from

$$\frac{\Delta a}{a} = -\left(2.22\sqrt{\frac{1}{\cosh k_0 h}}\frac{\Delta_B}{h}\frac{K_0 h}{\sinh k_0 h} + 1.11\frac{\Delta_S}{b}\left(1+\sqrt{\frac{1}{\cosh k_0 h}}\right)\right)\frac{\sqrt{g a}}{U}, \tag{3.2}$$

where Δ_B is the gap between the wavemaker and the bottom, Δ_S is the gap between the sidewalls and the wavemaker, b is the width of the wave tank, U is the wavemaker velocity and g is the gravity acceleration.

In this work, the numerical paddle displacement was calculated applying the wave height reduction model proposed by Madsen [38]. During the physical tests at CIEMito, Δ_B was 0.012 m and Δ_S 0.010 m. Employing Madsen [38] model for these conditions, we obtain a reduction on the generated wave height of 8.2% for wave case 1 and 8.9% for wave case 2. These reductions rates were then applied to the numerical paddle displacement. Figure 2 shows the paddle displacement used in the physical and numerical wave flumes for wave case 1.

Figure 3 is a snapshot of horizontal velocities in the numerical flume for four different time steps and for wave case 1. At the last two snapshots, the paddle is no longer moving and is possible to see how the wave overtops the structure and the horizontal velocities increase over the structure due to the reduction of the water column (depth).

For wave case 1, we compare in Figure 4 the free surface evolution obtained in the numerical flume with the corresponding ones obtained in the physical flume. For this wave case, the numerical flume reproduces accurately the nonlinear effects of wave generation, wave propagation, and wave reflection induced by the low-crested structure (captured at wave gauges WG0, WG1, WG2, and WG3 in Figure 4).

The two main overtopping events registered in the lab are also detected in the numerical flume (WG4 and WG5). The first and the last overtopping events are due to the ramp waves and were not detected in the numerical flume. These two minor overtopping events correspond to a flow over the structure that in the lab reached a maximum water lever at

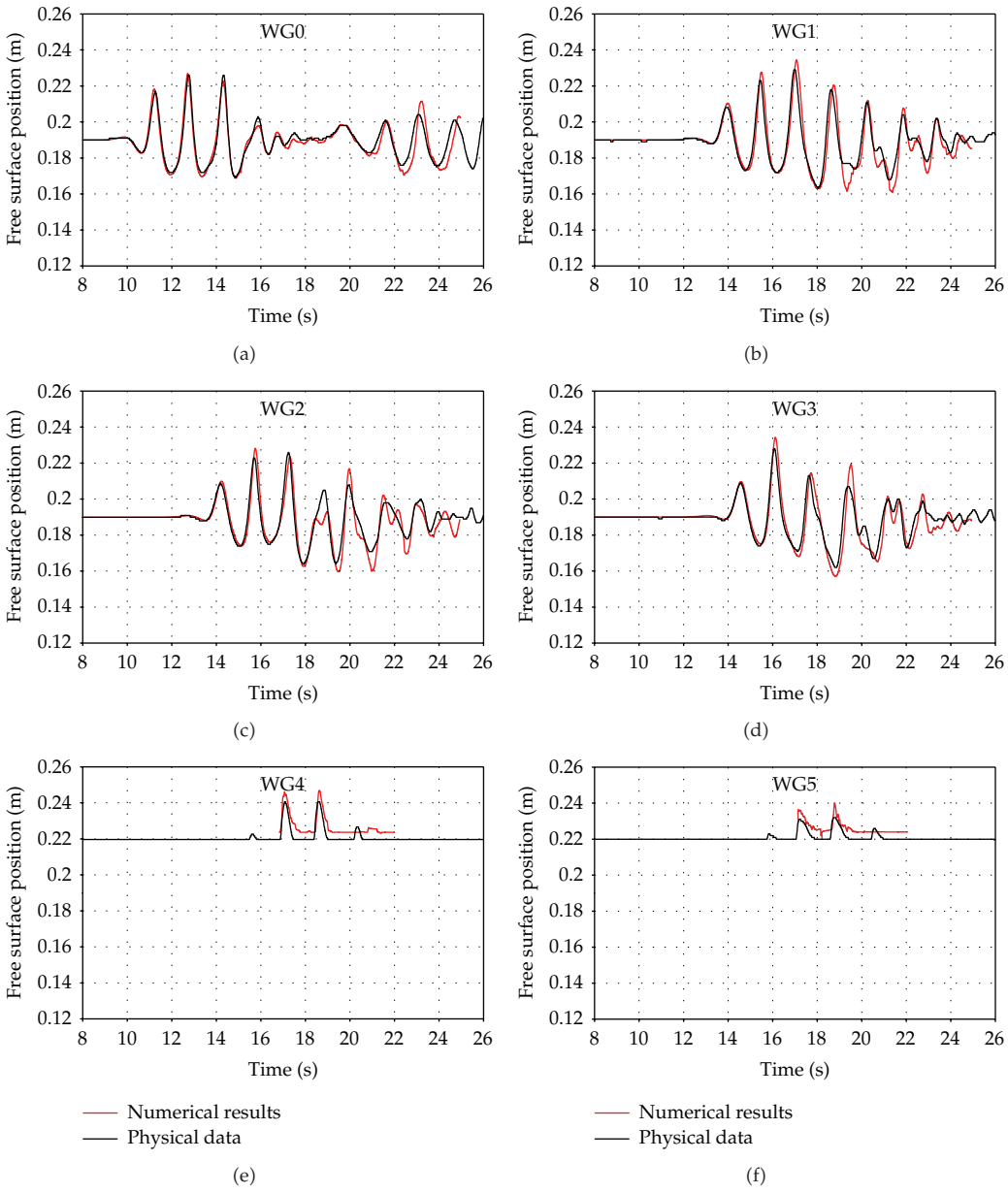

Figure 4: Numerical and physical free surface comparison at six different locations, all of them corresponding to wave case 1 defined by $H = 0.06$ m and $T = 1.55$ s.

WG4 which is smaller than 0.005 m. This value is below the numerical resolution in this zone as well as being close to the minimum free surface physical sensor accuracy. For the two main overtopping events, the numerical flume reproduces quite well the free surface evolution at both free surface sensors located over the structure (WG4 and WG5). The reduction from WG4 to WG5 of the maximum water level reached by the water flow is also well simulated

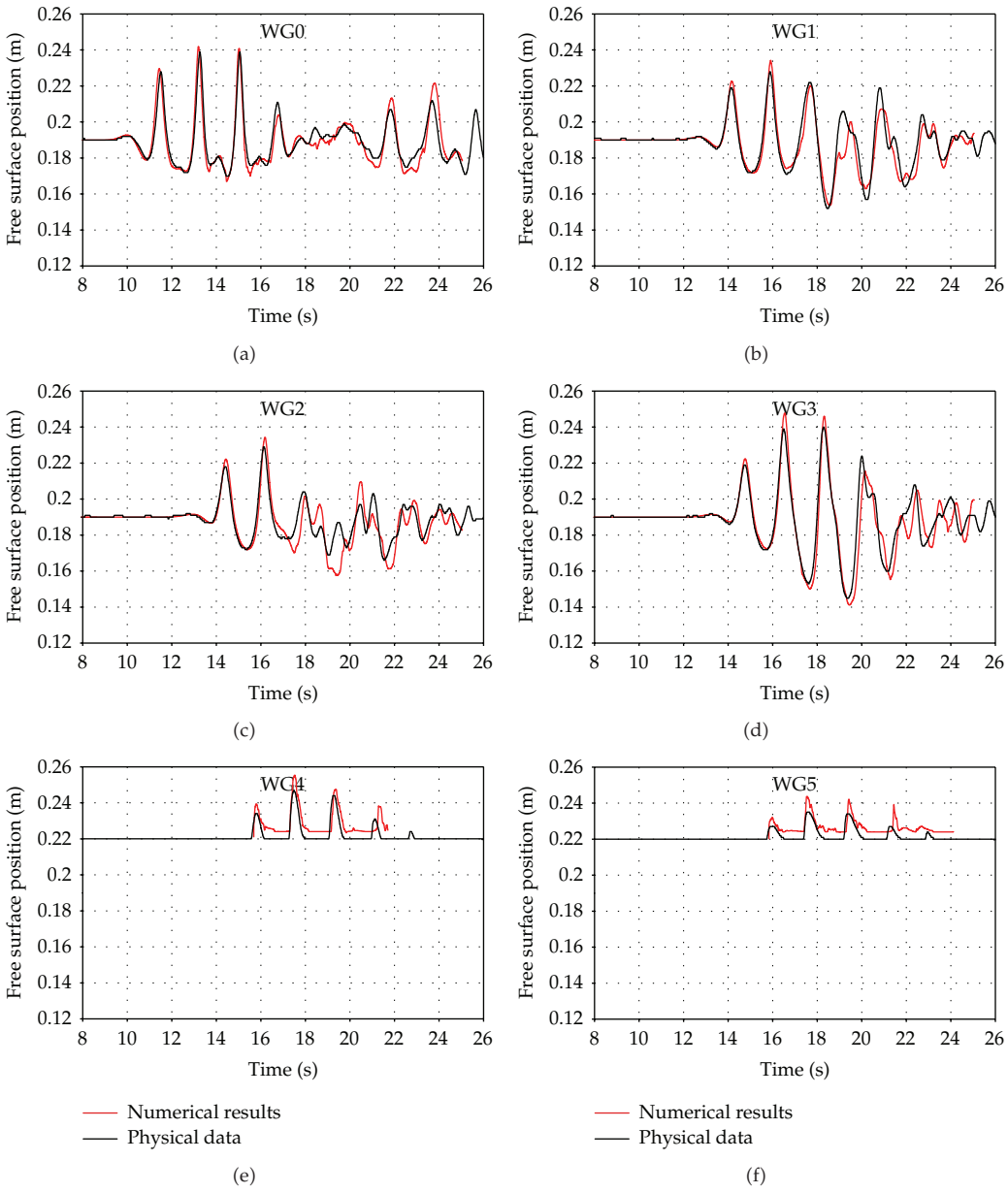

Figure 5: Numerical and physical free surface comparison at six different locations, all of them for wave case 2 defined by $H = 0.07$ m and $T = 1.8$ s.

numerically. A small overestimation of the maximum level reached by the flow over the structure is observed in the numerical flume.

In Figure 4, the constant water levels obtained after the described wave events at WG4 and WG5 correspond in the numerical flume to particles that remain stopped over the structure and therefore can be detected by the numerical free surface sensor. The constant levels equal to 0.005 m correspond to no flow conditions over the structure.

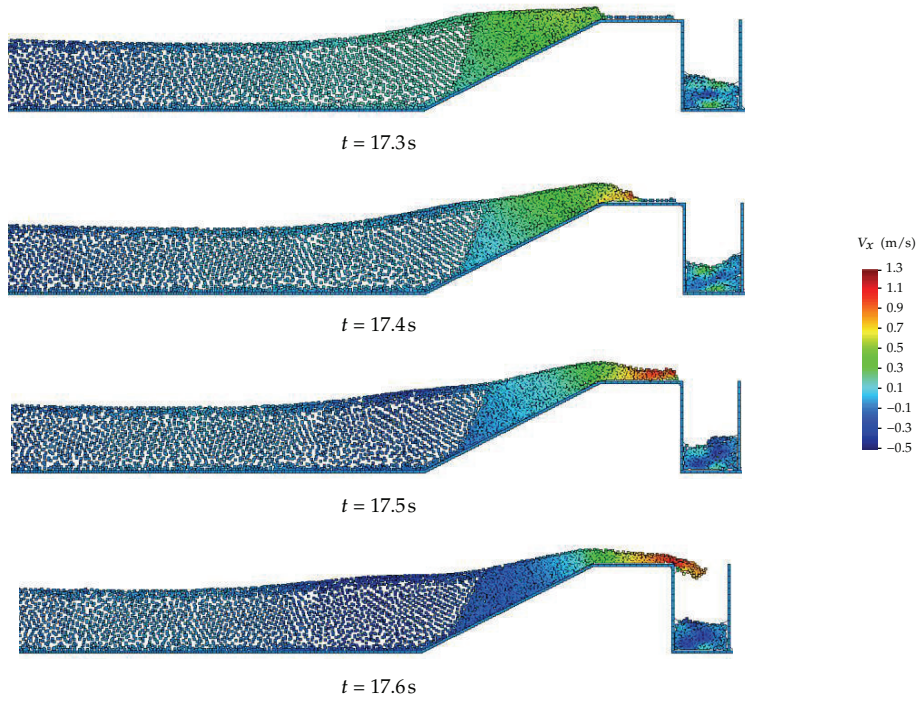

Figure 6: Horizontal velocities (m/s) close to the low-crested structure for four different time steps all corresponding to wave case 2 defined by $H = 0.07$ m and $T = 1.80$ s.

For wave case 2, we compare in Figure 5 the free surface evolutions obtained in the numerical flume with the corresponding ones registered in the lab. As it happened for wave case 1, the numerical flume in case 2 reproduces accurately the nonlinear effects of wave generation, wave propagation, and wave reflection from the low-crested structure (captured at wave gauges WG0, WG1, WG2, and WG3 in Figure 5).

A small overestimation in the maximum water level in WG4 and WG5 can be observed. The numerical flume can accurately predict the increase from wave case 1 to wave case 2 of the amount of water that overtops the structure.

One advantage of a numerical wave flume based on PFEM is the facility to obtain different result parameters such as velocities or pressure at all computational domain points. Figure 6 shows for wave case 2 the horizontal velocities around the structure for four consecutive instants during an overtopping event. In this figure, it is possible to see how the maximum water level decreases along the crest of the structure, inducing an increase of the maximum horizontal water velocity. At the middle and right end of the structure, the horizontal velocities reach values close to 1.3 m/s.

In Figure 7, some pictures taken in the lab, close to the structure, during an overtopping event for wave case 2 are compared with numerical results. In this figure, we can see that the numerical flume reproduces quite well the spatial and time evolution of the free surface around the structure during the overtopping event.

Although no physical velocity data is available, the good performance of the numerical model to reproduce free surface elevation evolution suggests acceptable results for other variables such as water velocity.

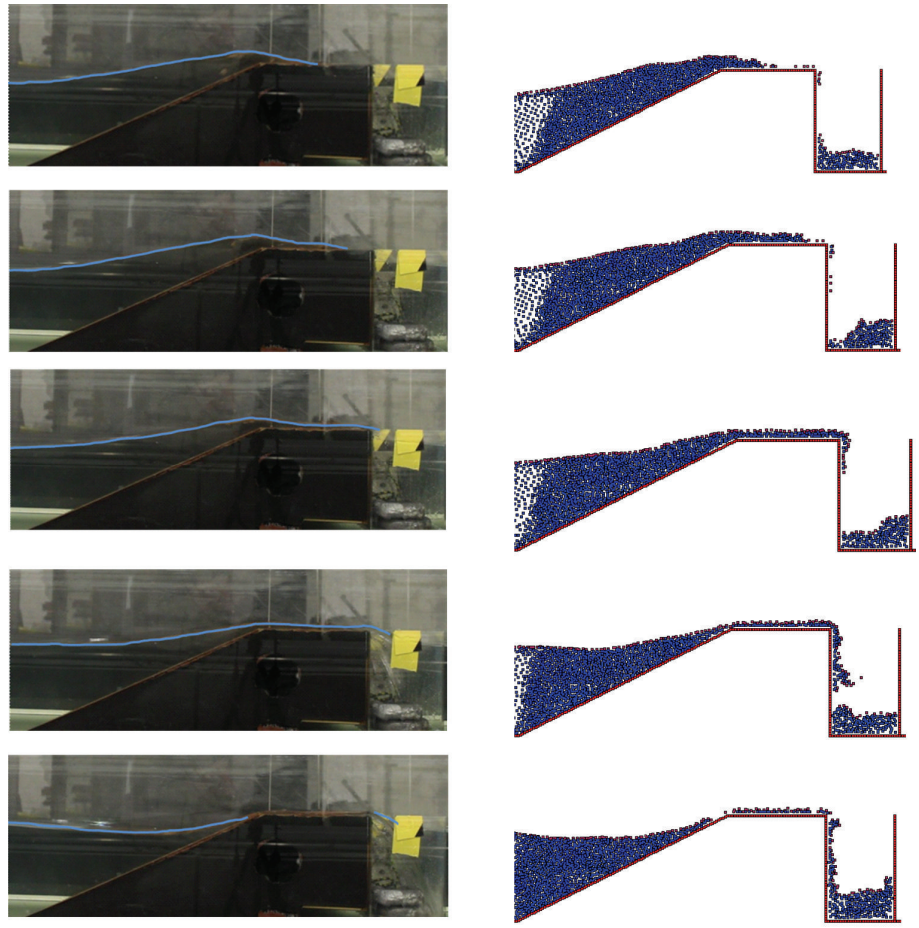

Figure 7: Visual comparison of one overtopping event obtained in the physical and numerical flume. The simulated case correspond to wave case 2, defined by $H = 0.07$ m and $T = 1.8$ s.

4. Overtopping for Breaking Waves

The ability of a numerical wave flume, based on the PFEM, to simulate the overtopping of maritime structures by breaking waves was also analyzed and tested in this work. State-of-the-art physical experiments for which results are free available online at the Refined Wave Measurements Database of the International Association for Hydraulic Research (IAHR) were simulated for this propose in our numerical flume.

The physical experiments were carried out by Stansby and Feng [39] in a small-scale wave flume and simulated regular waves overtopping an impermeable trapezoidal obstacle placed on a sloping beach. The beach slope is 1 : 20, and the trapezoidal structure has slopes of 1 : 2 both on the seaward and landward side with 0.2 m as horizontal crest width. The flume used in the experiments is 13 m long, 0.3 m wide, and 0.5 m deep. A piston type wave paddle with almost sinusoidal motion was used to generate regular waves of wave period $T = 2.39$ s and a surf similarity parameter ξ of about 0.3, where $\xi = S/\sqrt{H/L}$, S being the beach slope and the wave height given by H and wave length given by L. These wave

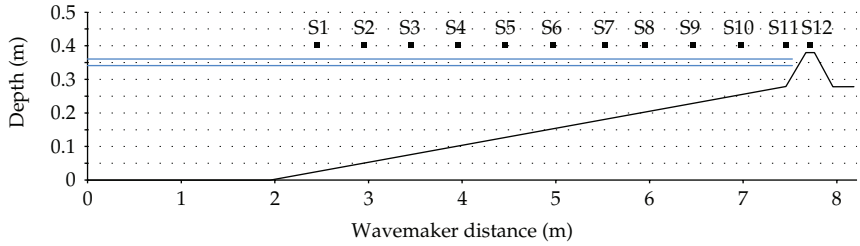

Figure 8: Sketch of the flume for the Stansby and Feng [32] tests.

parameters are values at the toe of the beach slope. Two different still water levels at the wavemaker, 0.36 m and 0.34 m, respectively, were tested. Stansby and Feng [39] measured the water surface elevation at 12 points along the flume using sensors with a resolution of about 0.5 mm. The geometry of the experimental configuration and water surface elevation deployment is indicated in Figure 8.

Stansby and Feng [39] experiments were simulated in a numerical wave flume based on the 2DV Navier-Stokes equations solved by the PFEM. As in the previous case (overtopping of nonbreaking waves at low-crested structure), to discretize the flume domain, two different nodal distances have been considered. In the first 6.5 m of the flume length a 0.01 m nodal distance was applied. For the other part of the domain, a 0.005 m distance between nodes was considered. This domain discretization leads to an initial finite elements mesh of 26875 and 24569 nodes for the still water level of 0.36 m and 0.34 m, respectively. The maximum time step used in the simulations was 0.001 s. The numerical tests were run on a 2.67 GHz Intel Core i7 CPU920, and the average execution time was about 85 hours for 35.4 s simulated.

Other time and mesh resolutions were tested in order to evaluate the computational time and the accuracy of the results along the flume. It was found that the accuracy of the overtopping results decreases substantially for nodal distances around the structure greater than 0.005 m.

A numerical piston paddle, with sinusoidal movement calculated by 3.1, was used to generate the waves. To calibrate the wave generation process, a set of simulations with different wave heights and wave period $T = 2.39$ s were run for the still water level of 0.36 m. It was found that wave height $H = 0.089$ m was the one that best fits the waves obtained in the experiments at the free surface sensor S1. The same paddle movement was used for both still water level cases.

Figure 9 is a snapshot of horizontal velocities for four different time steps and for the 0.36 m still water depth case. In this figure, we can see how the numerical flume is reproducing wave breaking and overtopping.

Figures 10 and 11 compare the free surface elevations obtained in the numerical and physical flumes for the still water level 0.36 m and 0.34 m cases, respectively. Graphics in these figures correspond to measured data and numerical results obtained with probes S1, S4, S6, S8, S11, and S12 that are located at 2.470 m, 3.970 m, 4.970 m, 5.964 m, 7.468 m, and 7.718 m away from the paddle, respectively.

Generally speaking, the water free surface evolution is well reproduced at the six probes. These results indicate that wave generation, shoaling, breaking, reflection, and overtopping processes are reproduced with an acceptable level of accuracy by the numerical

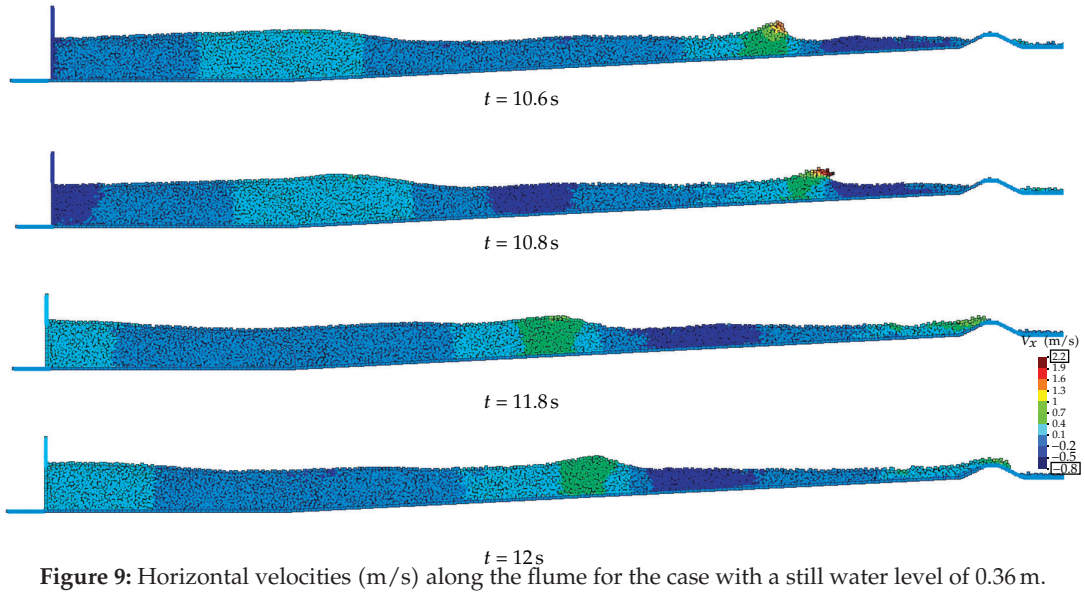

Figure 9: Horizontal velocities (m/s) along the flume for the case with a still water level of 0.36 m.

model for both mean water level cases. Although overtopping events are well detected by the numerical flume, the maximum water level reached by the flow over the structure is overestimated.

The differences observed between the physical and numerical free surfaces are attributed to the limits in accuracy of the numerical simulation for the complex physical processes involved (wave breaking turbulence, friction, etc.). However, we should notice that the nonexact reproduction of the boundary condition at the paddle can induce some distortion on the results.

5. Conclusions

A fully nonlinear numerical wave flume, based on the PFEM, has been developed to investigate the interaction of waves and maritime structures. Special efforts have been undertaken to improve the ability to simulate the actual (physical) flume with emphasis on the control of boundary conditions.

We have also defined and proposed a well-defined benchmark test case to study wave overtopping of regular nonbreaking waves at a simple low-crested maritime structure. This case has been tested in a small-scale physical flume and in a numerical flume based on the PFEM. Comparing physical data with numerical results, an assessment of the performance and robustness of the numerical flume has been carried out. The results show that for the two wave conditions tested the numerical flume reproduced with accuracy the nonlinear processes controlling the benchmark test proposed, such as nonlinear wave generation, energy losses along propagation and overtopping. The complex time and spatial evolution of the flux over the structure induced by overtopping events were well captured by the numerical simulations.

The Madsen [38] model to estimate the reduction of the generated wave height due to the leakage around the piston was successfully applied to calibrate wave generation in the numerical flume.

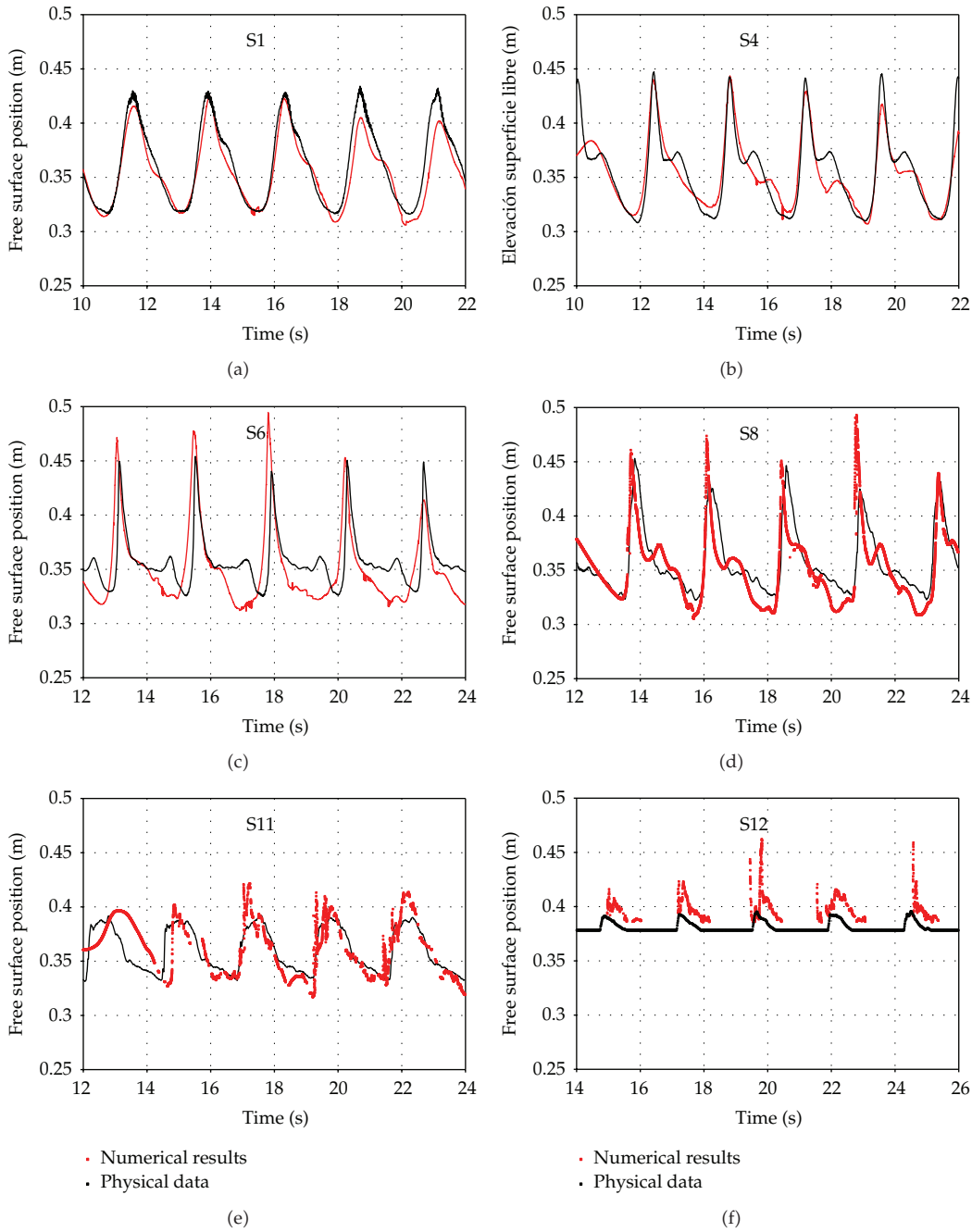

Figure 10: Numerical and physical free surface comparison at six different locations, corresponding to the case with a still water level of 0.36 m.

Depending on the scale and energy of the physical processes appearing along the flume, different mesh resolutions should be used along the calculation domain. Consequently, a nonfixed spatial resolution was applied, with good results for wave overtopping. This has allowed reducing the computational time effort.

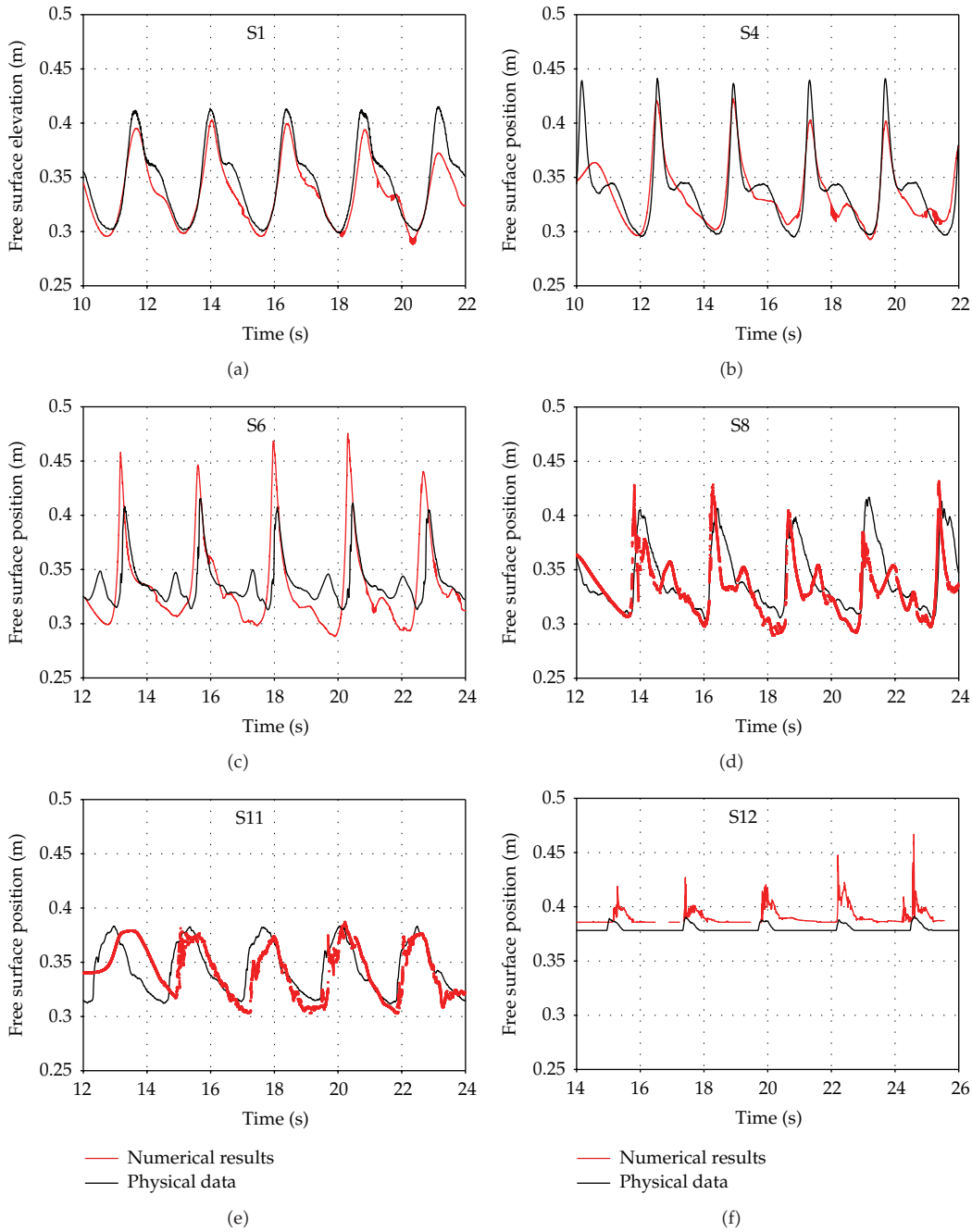

Figure 11: Numerical and physical free surface comparison at six different locations, corresponding to the case with a still water level of 0.34 m.

State-of-the-art physical experiments of regular waves overtopping for breaking conditions at an impermeable trapezoidal obstacle placed on a sloping beach have also been simulated with acceptable accuracy and robustness in the numerical wave flume based on the PFEM.

The results obtained for both breaking and nonbreaking waves indicate that a compromise has to be made between accuracy and computational efforts when selecting the time and space domain discretizations.

Overtopping events are typically defined by the mean discharge obtained at the back of the structure. However, we have shown in this paper that the shape of the flow over the structure induced by wave overtopping can lead to high velocity values that produce damages on maritime structures or even the loss of life. The results obtained in this work indicate that a numerical wave flume based on the PFEM can be applied as a complementary tool to physical models and semiempirical formulations to deal with overtopping studies of maritime structures. However, a compromise has to be made between the accuracy and validity field of each calculation tool, suggesting the use of one or other or even a hybrid modeling approach.

Acknowledgments

The authors wish to thank the UPC/CIEM lab team members Joaquim Sospedra and Andrea Marzeddu for their help in undertaking model tests. This research work was partly financed by the FP7 EU research project Hydralab IV (Contract no. 261520). The first author gratefully acknowledges the doctoral scholarship provided by "Fundação para a Ciência e Tecnologia," Contract no. SFRH/BD/44020/2008, funded by the European Social Fund and the Portuguese Ministry of Science, Technology and Higher Education.

References

[1] M. W. Owen, "Design of sea walls allowing for wave overtopping," Tech. Rep. number EX 924, Hydraulics Research, Wallingford, UK, 1980.

[2] L. Franco, M. de Gerloni, and J. W. van der Meer, "Wave overtopping on vertical and composite breakwaters," in *Proceedings of the 24th International Conference on Coastal Engineering*, pp. 1030–1045, ASCE, New York, NY, USA, October 1994.

[3] J. Pedersen, *Wave forces and overtopping on crown walls of rubble mound breakwaters—an experimental study [Ph.D. thesis]*, Hydraulic & Coastal Engineering Laboratory, Department of Civil Engineering, Aalborg University, Aalborg, Denmark, 1996.

[4] J. van der Meer, T. Pullen, W. Allsop, T. Bruce, H. Schüttrumpf, and A. Kortenhaus, "Prediction of overtopping," in *Handbook of Coastal and Ocean Engineering*, Y. C. Kim, Ed., chapter 14, World Scientific, 2010.

[5] S. A. Hughes, *Phisical Models and Laboratory Techniques in Coastal Engineering*, vol. 7 of *Advanced Series on Ocean Engineering*, World Scientific, 1993.

[6] J. Pearson, T. Bruce, W. Allsop, and X. Gironella, "Violent wave overtopping-measurements at large and small scale," in *Proceedings of the 28th International Conference on Coastal Engineering*, pp. 2227–2236, ASCE, Cardiff, UK, 2002.

[7] J. De Rouck, "CLASH-D46," Final Report, Ghent University, Belgium, 2005.

[8] T. L. Andersen, *Hydraulic response of rubble mound breakwaters. Scale effects—Berm breakwaters [Ph.D. thesis]*, Department of Civil Engineering, Aalborg University, 2006.

[9] M. T. Reis, M. G. Neves, and T. Hedges, "Investigating the lengths of scale model tests to determine mean wave overtopping discharges," *Coastal Engineering Journal*, vol. 50, no. 4, pp. 441–462, 2008.

[10] M. R. A. van Gent, "The modelling of wave action on and in coastal structures," *Coastal Engineering*, vol. 22, no. 3-4, pp. 311–339, 1994.

[11] N. Dodd, "Numerical model of wave run-up, overtopping, and regeneration," *Journal of Waterway, Port, Coastal and Ocean Engineering*, vol. 124, no. 2, pp. 73–81, 1998.

[12] K. Hu, C. G. Mingham, and D. M. Causon, "Numerical simulation of wave overtopping of coastal structures using the non-linear shallow water equations," *Coastal Engineering*, vol. 41, no. 4, pp. 433–465, 2000.

[13] C. M. Lemos, *Numerical modelling of shallow water waves: application of the VOF technique and k-E turbulence model [Ph.D. thesis]*, Universitat Politècnica de Catalunya, Barcelona, Spain, 1990.

[14] M. R. A. van Gent, P. Tonjes, H. A. H. Petit, and P. van den Bosch, "Wave action on and in permeable structures," in *Proceedings of the 24th International Conference on Coastal Engineering. Part 1 (of 3)*, pp. 1739–1753, Kobe, Japan, October 1994.

[15] P. Lin and P. L. F. Liu, "A numerical study of breaking waves in the surf zone," *Journal of Fluid Mechanics*, vol. 359, pp. 239–264, 1998.

[16] J. L. Lara, N. Garcia, and I. J. Losada, "RANS modelling applied to random wave interaction with submerged permeable structures," *Coastal Engineering*, vol. 53, no. 5-6, pp. 395–417, 2006.

[17] J. J. Monaghan and A. Kos, "Solitary waves on a cretan beach," *Journal of Waterway, Port, Coastal and Ocean Engineering*, vol. 125, no. 3, pp. 145–154, 1999.

[18] R. A. Dalrymple and B. D. Rogers, "Numerical modeling of water waves with the SPH method," *Coastal Engineering*, vol. 53, no. 2-3, pp. 141–147, 2006.

[19] S. Shao, C. Ji, D. I. Graham, D. E. Reeve, P. W. James, and A. J. Chadwick, "Simulation of wave overtopping by an incompressible SPH model," *Coastal Engineering*, vol. 53, no. 9, pp. 723–735, 2006.

[20] S. Koshizuka, A. Nobe, and Y. Oka, "Numerical analysis of breaking waves using the moving particle semi-implicit method," *International Journal for Numerical Methods in Fluids*, vol. 26, no. 7, pp. 751–769, 1998.

[21] T. C. A. Oliveira, F. X. Gironella, A. Sanchez-Arcilla, J. P. Sierra, and M. A. Celigueta, "Nonlinear regular wave generation in numerical and physical flumes," *Journal of Coastal Research*, no. SI 56, pp. 1025–1029, 2009.

[22] T. Pullen, N. W. H. Allsop, T. Bruce, A. Kortenhaus, H. Schüttrumpf, and J. W. van der Meer, "Overtopping manual, wave overtopping of sea defences and related structures: assessment manual," 2007, http://www.overtopping-manual.com.

[23] M. G. Neves, M. T. Reis, I. J. Losada, and K. Hu, "Wave overtopping of Póvoa de Varzim Breakwater: physical and numerical simulations," *Journal of Waterway, Port, Coastal and Ocean Engineering*, vol. 134, no. 4, pp. 226–236, 2008.

[24] P. L. F. Liu, P. Lin, K. A. Chang, and T. Sakakiyama, "Numerical modeling of wave interaction with porous structures," *Journal of Waterway, Port, Coastal and Ocean Engineering*, vol. 125, no. 6, pp. 322–330, 1999.

[25] D. E. Reeve, A. Soliman, and P. Z. Lin, "Numerical study of combined overflow and wave overtopping over a smooth impermeable seawall," *Coastal Engineering*, vol. 55, no. 2, pp. 155–166, 2008.

[26] I. J. Losada, J. L. Lara, R. Guanche, and J. M. Gonzalez-Ondina, "Numerical analysis of wave overtopping of rubble mound breakwaters," *Coastal Engineering*, vol. 55, no. 1, pp. 47–62, 2008.

[27] S. Shao, "Incompressible SPH simulation of wave breaking and overtopping with turbulence modelling," *International Journal for Numerical Methods in Fluids*, vol. 50, no. 5, pp. 597–621, 2006.

[28] H. Gotoh, H. Ikari, T. Memita, and T. Sakai, "Lagrangian particle method for simulation of wave overtopping on a vertical seawall," *Coastal Engineering Journal*, vol. 47, no. 2-3, pp. 157–181, 2005.

[29] S. R. Idelsohn, E. Oñate, and F. Del Pin, "A Lagrangian meshless finite element method applied to fluid-structure interaction problems," *Computers and Structures*, vol. 81, no. 8-11, pp. 655–671, 2003.

[30] E. Oñate, F. Del Pin, and R. Aubry, "The particle finite element Method. an overview," *International Journal of Computational Methods*, vol. 1, no. 2, pp. 267–307, 2004.

[31] E. Oñate, S. R. Idelsohn, M. A. Celigueta, and R. Rossi, "Advances in the particle finite element method for the analysis of fluid-multibody interaction and bed erosion in free surface flows," *Computer Methods in Applied Mechanics and Engineering*, vol. 197, no. 19-20, pp. 1777–1800, 2008.

[32] R. Codina, "Pressure stability in fractional step finite element methods for incompressible flows," *Journal of Computational Physics*, vol. 170, no. 1, pp. 112–140, 2001.

[33] E. Oñate, "A stabilized finite element method for incompressible viscous flows using a finite increment calculus formulation," *Computer Methods in Applied Mechanics and Engineering*, vol. 182, no. 3-4, pp. 355–370, 2000.

[34] S. R. Idelsohn, N. Calvo, and E. Onate, "Polyhedrization of an arbitrary 3D point set," *Computer Methods in Applied Mechanics and Engineering*, vol. 192, no. 22-23, pp. 2649–2667, 2003.

[35] S. R. Idelsohn, E. Oñate, N. Calvo, and F. Del Pin, "The meshless finite element method," *International Journal for Numerical Methods in Engineering*, vol. 58, no. 6, pp. 893–912, 2003.

[36] H. Edelsbrunner and E. P. Mucke, "Three-dimensional alpha-shape," *ACM Transactions on Graphics*, vol. 3, pp. 43–72, 1994.

[37] F. Biésel and F. Suquet, "Les appareils générateurs de houle en laboratoire," *La Houille Blanche*, vol. 6, no. 2, pp. 147–165, 1951.
[38] O. S. Madsen, "Waves generated by a piston- type wavemaker," vol. 1, pp. 589–607, 1970.
[39] P. K. Stansby and T. Feng, "Surf zone wave overtopping a trapezoidal structure: 1-D modelling and PIV comparison," *Coastal Engineering*, vol. 51, no. 5-6, pp. 483–500, 2004.